⟨Original⟩

A Predictor-Corrector Algorithm of the Generalized-α Method for Analysis of Structural Dynamics

동적해석을 위한 일반화된 α 방법의 예측-수정자 알고리즘

정 진 태* · Gregory M. Hulbert**

Jintai Chung and Gregory M. Hulbert

ABSTRACT

A new predictor-corrector explicit time integration algorithm is presented for solving structural dynamics problems. The basis of the algorithm is the implicit generalized-α method recently developed by the authors. Like its implicit parent, the explicit generalized-α method is a one-parameter family of algorithms in which the parameter defines the high-frequency numerical dissipation. The algorithm can be utilized effectively for linear and nonlinear structural dynamics calculations in which numerical dissipation is needed to reduce spurious oscillations inherent in non-dissipative time integration methods used to solve wave propagation problems.

요 약

본 논문에서 구조동력학 문제를 풀기 위한 명시적(explicit) 예측-수정자 시간적분법을 개발하였으며, 이 알고리즘은 최근 개발된 암시적(implicit) 일화화된 α 방법으로부터 유도하였다. 암시적 방법과 같이 명시적 일반화된 α 방법도 하나의 변수를 갖는 알고리즘의 집합이며, 이 변수는 고주파 영역에서 수치감쇠의 양을 정의한다. 제안된 알고리즘은 수치감쇠가 없는 시간적분법으로 파의 전달 문제를 풀 때 나타나는 가상의 진동을 감소시키는 수치감쇠를 가지고 있기 때문에 선형 혹은 비선형의 구조동력학 문제에 효과적으로 이용될 수 있다.

1. Introduction

Numerous efforts during the past several decades

*Member, Space R & D Division, Korea Aerospace Research Institute
**Department of Mechanical Engineering and Applied Mechanics, The University of Michigan, Ann Arbor

have focused on developing implicit time integration algorithms for structural dynamics that include controllable numerical dissipation in the high frequency response domain. The purpose of the numerical dissipation is to reduce the spurious, nonphysical oscillations that may occur due to excitation of spatially unresolved modes. The basic difficulty designing such algorithms is to add high-frequency

dissipation without introducing excessive algorithmic damping in the important low-frequency modes. Numerous dissipative algorithms have been developed that attain high-frequency dissipation with little low-frequency dissipation while maintaining second-order accuracy : e. g., the Wilson-θ method,[1] the HHT-α method of Hiber, Hughes and Taylor,[2] the WBZ-α method of Wood, Bossak and Zienkiewicz,[3] the ρ method of Bazzi and Anderheggen[4] and the θ_1-method of Hoff and Phal.[5,6] The authors showed that good accuracy can be achieved even if the spurious root does not tend towards zero in the low-frequency limit.[7] This permits move flexibility in the design of time integration algorithms. Based on this theory, we developed a second-order accurate, implicit time integration algorithm that is optimal in the sense that for a given value of high-frequency dissipation, low-frequency dissipation is minimized.[8] This new algorithm, which we call the generalized-α method, is a one-parameter family of algorithms; the parameter directly specifies the amount of highfrequency dissipation of the algorithm. The algorithm can be directly implemented into standard programs with little additional effort beyond that required to implement the HHT-α or WBZ-α methods.

Numerical dissipation is also important (perhaps more important) when solving structural dynamics problems using explicit methods. The principal use of explicit time intergration methods is for problems in which the time step size needed for accuracy is of the same order as the step size limit dictated by the stability limit of an explicit method, e. g., wave propagation and impact problems. The responses of these problems usually are characterized by large gradients or discontinuities in the solution due to the propagating wave front. It is well known that dissipative mechanisms are needed to reduce or eliminate oscillations in solutions that exhibit discontinuities unless front tracking methods or discontinuous solution fields are employed. Amongst explicit time integration methods for structural dynamics, the nearly universal choice is the central difference (CD) method which possesses no numerical dissipation. If a mesh is constructed so that the critical time step

limit for each element is the same, results from the CD method are nearly optimal. This behavior is best illustrated by the impact of a ond-dimensional, uniform elastic bar; the CD method computes the exact solution when a uniform spatial mesh is employed. However, in practical computations, it is not feasible to construct a mesh so that the critical time step limit is the same for all elements. The consequence is that oscillations occur in the solutions computed using the CD method. An explicit time integration algorithm for structural dynamics that possesses numerical dissipation was developed by Miranda, Ferencz and Hughes[9] based upon the implicit HHT-α method. The explicit and implicit α methods were then combined into a unified implicit-explicit scheme that was shown to provide improved solutions compared to the implicit-explicit method developed by Hughes and Liu[10,11] based upon the Newmark method. The authors developed an implicit single-step version of the Houbolt method and its predictor-corrector algorithm which are merged into an implicit-explicit method.[12] On the other hand, Chung and Lee[13] recently proposed an explicit method which is second-order accurate and completely explicit even when the damping matrix is not diagonal in linear structural dynamics or the internal force vector is a function of velocities in nonlinear structural dynamics.

In this paper we present a predictor-corrector explicit time integration algorithm that has numerical dissipation as its implicit parent of the generalized-α method. Similar to its parent, the explicit generalized-α method was designed so that for a given value of high-frequency dissipation, the low-frequency dissipation is minimized.

2. Implicit Generalized-α Method

For completeness, we present the implicit generalized-α method below. This algorithm is second-order accurate and unconditionally stable when solving linear structural dynamics problems. The basic form of the generalized-α method is :

$$Ma_{n+1-a_m} + Cv_{n+1-a_f} + Kd_{n+1-a_f} = F(t_{n+1-a_f}) \tag{1}$$

$$d_{n+1} = d_n + \Delta t v_n + \Delta t^2 \left(\left(\frac{1}{2} - \beta\right) a_n + \beta a_{n+1}\right) \tag{2}$$

$$v_{n+1} = v_n + \Delta t ((1-\gamma) a_n + \gamma a_{n+1}) \tag{3}$$

$$d_0 = d \tag{4}$$

$$v_0 = v \tag{5}$$

$$a_0 = M^{-1}(F(0) - Cv - Kd) \tag{6}$$

where

$$d_{n+1-a_f} = (1-\alpha_f) d_{n+1} + \alpha_f d_n \tag{7}$$

$$v_{n+1-a_f} = (1-\alpha_f) v_{n+1} + \alpha_f v_n \tag{8}$$

$$a_{n+1-a_m} = (1-\alpha_m) a_{n+1} + \alpha_m a_n \tag{9}$$

$$t_{n+1-a_f} = (1-\alpha_f) t_{n+1} + \alpha_f t_n \tag{10}$$

in which $n \in \{0, 1, \cdots, N-1\}$, N is the number of time steps, $\Delta t = t_{n+1} - t_n$ is the time step and d and v are prescribed initial data. In terms of the desired high-frequency dissipation ρ_∞, the algorithmic parameters are given by

$$\alpha_m = \frac{2\rho_\infty - 1}{\rho_\infty + 1}, \quad \alpha_f = \frac{\rho_\infty}{\rho_\infty + 1} \tag{11}$$

$$\gamma = \frac{1}{2} - \alpha_m + \alpha_f, \quad \beta = \frac{1}{4}(1 - \alpha_m + \alpha_f)^2 \tag{12}$$

See Reference 8 for the derivation, accuracy and stability of the implicit generalized-α method.

3. Predictor-Corrector Explicit Form of the Implicit Generalized-α Method

Following the strategy taken to develop predictor-corrector explicit (PCE) methods for the Newmark and HHT-α methods, a PCE implementation of the implicit generalized-α method has the form:

Predictors:

$$\tilde{d}_{n+1} = d_n + \Delta t v_n + \left(\frac{1}{2} - \beta\right)\Delta t^2 a_n \tag{13}$$

$$\tilde{v}_{n+1} = v_n + (1-\gamma)\Delta t a_n \tag{14}$$

Balance equation:
$$(1-\alpha_m) M a_{n+1} = (1-\alpha_f)(F_{n+1} - K\tilde{d}_{n+1}) + \alpha_f(F_n - Kd_n) - \alpha_m M a_n \tag{15}$$

Correctors:

$$d_{n+1} = \tilde{d}_{n+1} + \beta \Delta t^2 a_{n+1} \tag{16}$$

$$v_{n+1} = \tilde{v}_{n+1} + \gamma \Delta t a_{n+1} \tag{17}$$

where α_m, α_f, β and γ are given by (11)~(12). In contrast to the implicit generalized-α method, ρ_∞ is

no longer the value of the spectral radius in the high-frequency limit for the above explicit version. This may be seen clearly in Fig. 1 which shows the variation in spectral radius as a function of ρ_∞. With $\rho_\infty = 0$, the algorithm has no numerical dissipation while the implicit generalized-α method is asymptotically annihilating when $\rho_\infty = 0$. When $\rho_\infty = 1$, the algorithm is *unstable*. An expression for the stability limit for the algorithm is given by

$$\Omega_c = \sqrt{\frac{12(1-\rho_\infty)(1+\rho_\infty)^2}{3 + 3\rho_\infty - 3\rho_\infty^2 + \rho_\infty^3}} \tag{18}$$

where the c subscript is used to denote the critical limit and $\Omega = \omega\Delta t$ in which ω denotes the maximum system eigenvalue. As shown in Fig. 2, the stability limit of the PCE implementation decreases as ρ_∞ increases. Thus, unlike the PCE forms developed for the Newmark and HHT-α algorithms, the
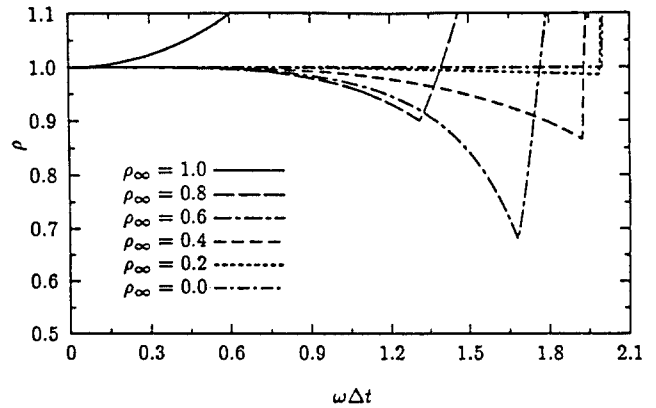

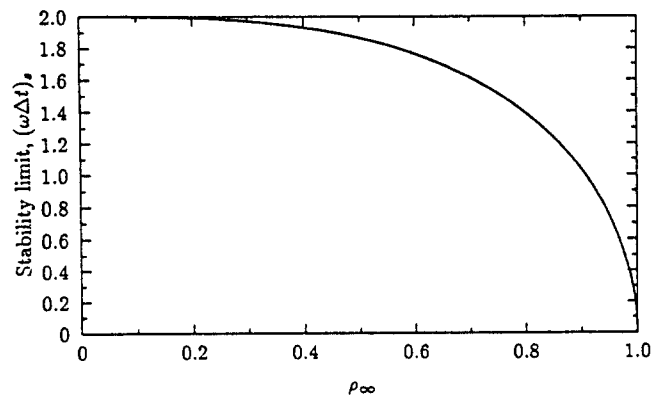**Fig. 1** Spectral radius of the predictor-corrector form of the implicit generalized-α method

Fig. 2 Stability limit of the predictor-corrector from of the implicit generalized-α method

generalized-α method does not admit a PCE form in which the same parametric relations as the implicit parent can be used.

4. The Explicit Generalized-α Method

To obtain a useful explicit generalized-α (EG-α) method, we relax the restrictions (11)~(12) and derive new relationships for the algorithmic parameters. To do so, we recall how the implicit generalized-α method was developed. The implicit generalized-α method was constructed by requiring the three roots of the algorithm's characteristic equation to be real and equal in the high-frequency limit. To maximize high-frequency dissipation, the two principal roots remain complex conjugate except in the high-frequency limit. That is, the principal roots bifurcate only in the high-frequency limit. For an explicit method, the notion of high-frequency limit is replaced by the critical limit, Ω_c. Since root bifurcation results in a decrease in high-frequency dissipation, there is two limits of concern for an explicit method : Ω_c and the bifurcation limit, denoted by Ω_b.

Let ρ_p and ρ_s denote the values of the principal and spurious roots, respectively, of the algorithm's characteristic equation at the bifurcation limit, Ω_b (actually the absolute values of the roots since the roots typically have negative values). In terms of ρ_p and ρ_s, the algorithmic parameters, Ω_b and Ω_c are given by

$$\alpha_m = \frac{2\rho_p\rho_s + \rho_p - 1}{(1 + \rho_p)(1 + \rho_s)} \tag{19}$$

$$\beta = \alpha_f + \frac{1 - \rho_p - 2\rho_p\rho_s}{(1 + \rho_p)(1 + \rho_s)}$$
$$+ \frac{(1 - \rho_p)(1 - \rho_p\rho_s)^2}{\alpha_f(1 + \rho_p)^2(1 + \rho_s)(2 + \rho_s - \rho_p\rho_s)} \tag{20}$$

$$\gamma = \frac{1}{2} - \alpha_m + \alpha_f \tag{21}$$

$$\Omega_b = \sqrt{(1 + \rho_p)(2 + \rho_s - \rho_p\rho_s)} \tag{22}$$

$$\Omega_c =$$

$$\sqrt{\frac{4(1 + \rho_p)(2 + \rho_s - \rho_p\rho_s)(3 - \rho_p + \rho_s - 3\rho_p\rho_s)}{2(5 - \rho_p^2) + (5 - 13\rho_p - \rho_p^2 + \rho_p^3)\rho_s - (1 - \rho_p)^3\rho_s^2}} \tag{23}$$

where the condition of γ is obtained by enforcing

second-order accuracy. The stability limit, (23), holds provided $\rho_b \neq 1$ or $\rho_s \neq 1$; when $\rho_p = \rho_s = 1$, then $\Omega_c = 2$. Note that in addition to ρ_p and ρ_s, α_f is also a free paremeter. For computational convenience, we let

$$\alpha_f = 1 \tag{24}$$

The characteristics of the EG-α method can be studied in terms of ρ_p and ρ_s. To maximize high-frequency numerical dissipation, we requiere $\rho_s \leq \rho_p$. One result of this constraint is that $\Omega_b \leq \Omega_c$. The variation in Ω_b as a function of ρ_p and ρ_s is depicted in Fig. 3. It can be seen that for a given value of ρ_p, Ω_b is maximum when $\rho_s = \rho_p$. A second consequence of enforcing $\rho_s \leq \rho_p$ is that the value of the spectral radius at the bifurcation limit is ρ_p. This may be seen in Fig. 4 which shows the variation in the spectral radius curve as a function of ρ_s for $\rho_p = 0.6$. Again note that the maximum value of Ω_b occurs
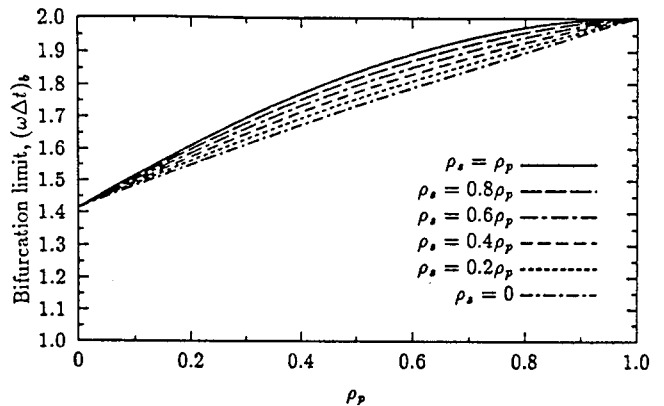

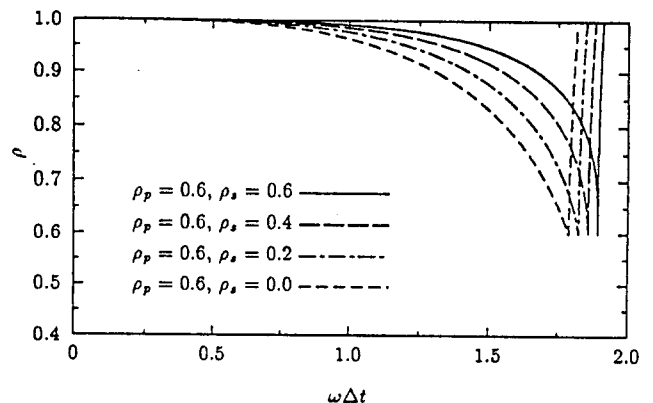**Fig. 3** Bifurcation limit variation of the explicit generalized-α method

Fig. 4 Spectral radius dependence on ρ_s for the explicit generalized-α method ($\rho_p = 0.6$)

when $\rho_s = \rho_p$. Fig. 4 also shows that the EG-α method is similar to the implicit generalized-α method in that for a given value of high-frequency dissipation, low-frequency dissipation is minimized when $\rho_s = \rho_p$. Denoting the value of the spectral radius at Ω_b by ρ_b, we have that $\rho_s = \rho_p = \rho_b$ achieves the optimal balance of low-frequency and high-frequency dissipation. What results is a one-parameter (ρ_b) family of the EG-α methods; the algorithm is summarized in Table 1.

The variation in spectral radius as a function of ρ_b is shown in Fig. 5. Note that when $\rho_b = 0$, the EG-α method possesses an explicit time integration algorithm's version of asymptotic annihilation. That is, provided that the critical time step is chosen based upon Ω_b, any high-frequency response of the structure will be nearly annihilated in one time step. The
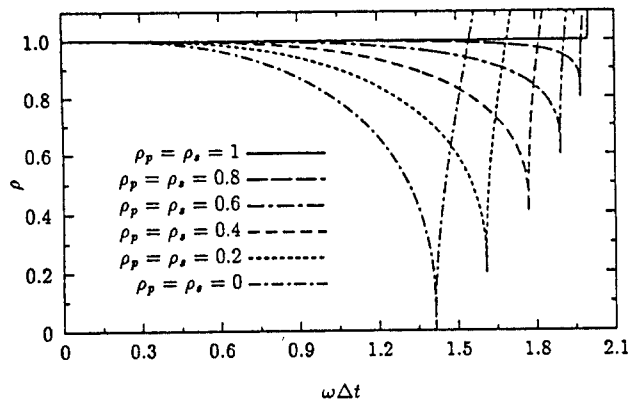
numerical damping ratio of the EG-α method is shown in Fig. 6 for different values of ρ_b; $\bar{\xi}$ denotes the numerical damping as a fraction of critical damping and T is the period of natural vibration. The numerical damping increases from zero when $\rho_b = 1$ to a maximum value when $\rho_b = 0$. The relative period error is shown in Fig. 7 where $\bar{T}$ denotes the numerical period. It is interesting to note that both period elongation and shortening can occur in the EG-α method depending on ρ_b. Period error is minimized in the low-frequency domain when $\rho_b = 0.367$.

5. Numerical Example

To demonstrate the effectiveness of the numerical dissipation inherent in the EG-α method, we con-
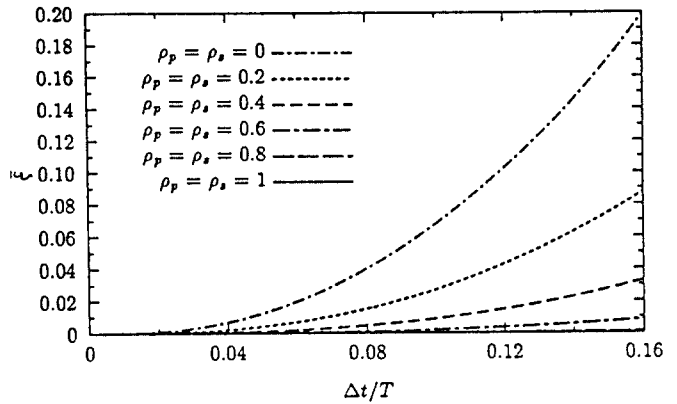

Fig. 5 Spectral radius dependence on ρ_b for the explicit generalized-α method

Fig. 6 Numerical damping ration of the explicit generalized-α method

Table 1 Explicit generalized-α algorithm

$$(1-\alpha_m)\,\boldsymbol{M}\boldsymbol{a}_{n+1} = \boldsymbol{F}_n - \boldsymbol{K}\boldsymbol{d}_n - \alpha_m \boldsymbol{M}\boldsymbol{a}_n$$

$$\boldsymbol{d}_{n+1} = \boldsymbol{d}_n + \varDelta t \boldsymbol{v}_n + \varDelta t^2\left(\left(\frac{1}{2}-\beta\right)\boldsymbol{a}_n + \beta\boldsymbol{a}_{n+1}\right)$$

$$\boldsymbol{v}_{n+1} = \boldsymbol{v}_n + \varDelta t\,((1-\gamma)\,\boldsymbol{a}_n + \gamma\boldsymbol{a}_{n+1})$$

$$\alpha_m = \frac{2\rho_b - 1}{1 + \rho_b}$$

$$\beta = \frac{5 - 3\rho_b}{(1+\rho_b)^2(2-\rho_b)}$$

$$\gamma = \frac{1}{2} - \alpha_m + \alpha_f$$

$$\Omega_b = (1+\rho_b)\sqrt{2-\rho_b}$$

$$\Omega_c = \sqrt{\frac{12(1+\rho_b)^3(2-\rho_b)}{10+15\rho_b - \rho_b^2 + \rho_b^3 - \rho_b^4}}$$
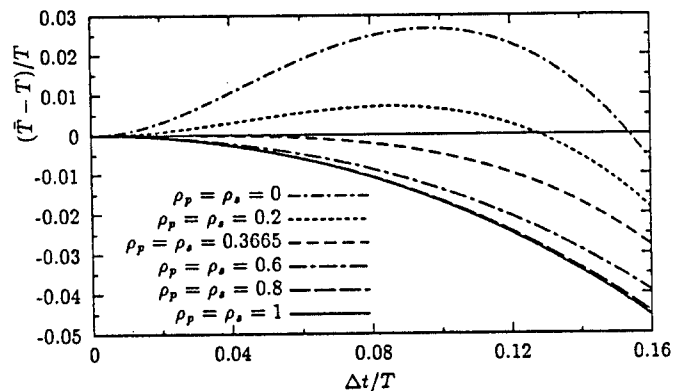

Fig. 7 Relative period error of the explicit generalized-α method

sider the impact of a one dimensional, homogeneous elastic rod with linearly varying cross-sectional area ; see Fig. 8. The bar is moving with an initial speed, v_0, when the left end impacts the rigid wall. The length of the bar (L) is 4 ; density, Young's modulus and v_0 have unit values ; the cross-sectional area is given by

$$A(x) = A_0 + \frac{A_L - A_0}{L} x \qquad (25)$$

where $A_0 = 1$ and $A_L = 0.01$ are the cross-sectional areas of the left and right ends, respectively and x is measured from the left end. Employing linear rod elements, the maximum element eigenvalue is given by

$$\omega_{max}^e = \frac{c(A_i + A_{i+1})}{h^e \sqrt{A_i A_{i+1}}} \qquad (26)$$

where c is the wave speed ; $c = \sqrt{E/\rho}$. Using the maximum eigenvalue of all elements as an upper bound to the maximum eigenvalue of the bar discretized by 400 elements, the critical time step, $\varDelta t_c$, for
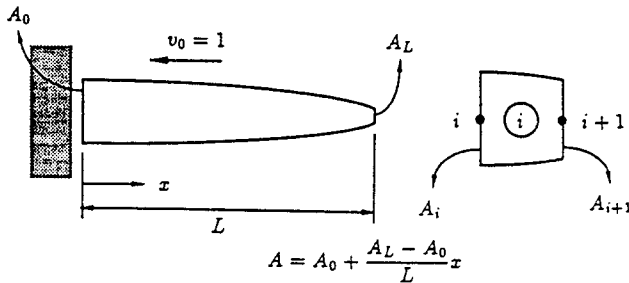

Fig. 8 Depiction of the tapered rod impact problem
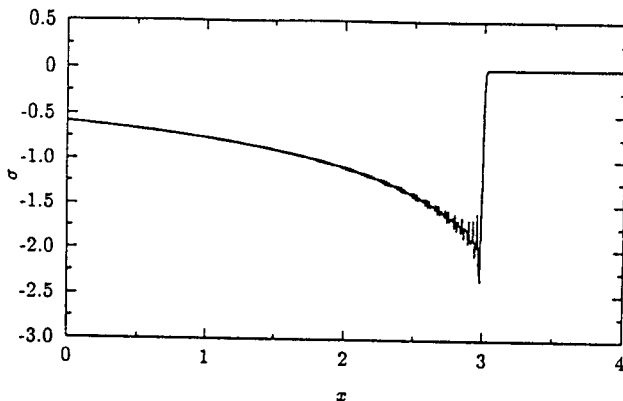

Fig. 9 Stress distribution in the tapered rod at $t_N = 3$ computed using the central difference method
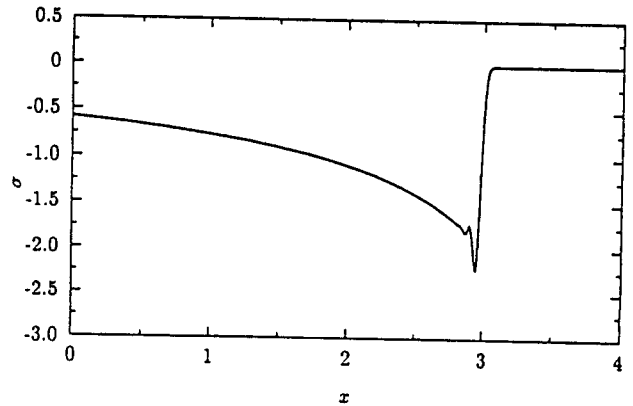

Fig. 10 Stress distribution in the tapered rod at $t_N = 3$ computed using the explicit generalized-α method

the CD method is $\varDelta t_c = 9.939 \times 10^{-3}$. For the EG-$\alpha$ method, we let $\rho_b = 0.6$; then $\varDelta t_c = 9.408 \times 10^{-3}$. Figs. 9 and 10 show the stress distribution in the rod for $t_N = 3$, computed using the CD and EG-α methods, respectively. It is clear from the figures that the spurious oscillations inherent in the CD method are reduced substantially by the EG-α method.

6. Conclusions

A predictor-corrector explicit version of the generalized-α (EG-α) method has been presented for structural dynamics. The disign and performance of the algorithm were described ; it was shown that an optimal combination of low-frequency and high-frequency dissipation can be obtained within a one-parameter family of algorithms. Unlike the predictor-corrector explicit methods developed for the Newmark and HHT-α methods, the algorithmic parameter definitions differ between the implicit and explicit generalized-α methods. The importance of the numerical dissipation inherent in the EG-α method was demonstrated by comparing its computed response with that of the central difference method for a simple model problem.

The development in this paper was specifically restricted to undamped systems. Adding physical damping presents both challenges and opportunities for the generalized-α methods ; this is the subject of a subsequent publication.

References

(1) Wilson, E. L., 1968, "A Computer Program for the Dynamic Stress Analysis of Underground Structure," SESM Report No. 68-1, Division of Structural Engineering and Structural Mechanics, University of California, Berkeley, CA.

(2) Hilber, H. M., Hugher, T. J. R. and Taylor, R. L., 1977, "Improved Numerical Dissipation for Time Integration Algorithms in Structural Dynamics," Earthquake Engineering and Structural Dyanmics, Vol. 5, pp. 283~292.

(3) Wood, W. L., Bossak, M. and Zienkiewicz, O. C., 1981, "An Alpha Modification of Newmark's Method," International Journal for Numerical Methods in Engineering, Vol. 15, pp. 1562~1566.

(4) Bazzi, G. and Anderheggen, E., 1982, "The ρ-Family of Algorithms for Time-Step Integration with Improved Numerical Dissipation," Earthquake Engineering and Structural Dynamics, Vol. 10, pp. 537~550.

(5) Hoff, C. and Phal, P. J., 1988, "Development of an Implicit Method with Numerical Dissipation from a Generalized Single-Step Algorithm for Structural Dynamics," Computer Methods in Applied Mechanics and Engineering, Vol. 67, pp. 367~385.

(6) Hoff, C. and Phal, P. J., 1988, "Practical Performance of the θ_1 Method and Comparison with Other Dissipative Algorithms in Structural Dynamics," Computer Methods in Applied Mechanics and Engineering, Vol. 67, pp. 87~110.

(7) Hulbert, G. M. and Chung, J., 1994, "The Unimportance of the Spurious Root of Time Integration Algorithms for Structural Dynamics," Communications in Numerical Methods in Engineering, Vol. 10, pp. 591~597.

(8) Chung, J. and Hulbert, G. M., 1993, "A Time Integration Algorithm for Structural Dynamics with Improved Numerical Dissipation : the Generalized-α Method," ASME Journal of Applied Mechanics, Vol. 60, pp. 371~375.

(9) Miranda, I., Ferencz, R. M. and Hughes, T. J. R., 1989, "An Improved Implicit-Explicit Time Integration Method for Structural Dynamics," Earthquake Engineering and Structural Dynamics, Vol. 18, pp. 643~653.

(10) Hughes, T. J. R. and Liu, W. K., 1978, "Implicit-Explicit Finite Elements in Transient Analysis : Stability Theory," ASME Journal of Applied Mechanics, Vol. 45, pp. 371-374.

(11) Hughes, T. J. R. and Liu, W. K., 1978, "Implicit-Explicit Finite Elements in Transient Analysis : Implementation and Numerical Examples," ASME Journal of Applied Mechanics, Vol. 45, pp. 375-378.

(12) Chung, J. and Hulbert, G. M., 1994, "A Family of Single-Step Houbolt Time Integration Algorithms for Structural Dynamics," Computer Methods in Applied Mechanics and Engineering, Vol. 118, pp. 1~11.

(13) Chung, J. and Lee, J. M., 1994, "A New Family of Explicit Time Integration Methods for Linear and Non-Linear Structural Dynamics," International Journal for Numerical Methods in Engineering, Vol. 37, pp. 3961~3976.